

Sunyaev-Zel'dovich Effect Imaging of Massive Clusters of Galaxies at Redshift > 0.8

Marshall Joy¹, Samuel LaRoque², Laura Grego³, John E. Carlstrom², Kyle Dawson⁴,
Harald Ebeling⁵, William L. Holzapfel⁴, Daisuke Nagai², & Erik D. Reese²

ABSTRACT

We present Sunyaev-Zel'dovich Effect (SZE) imaging observations of three distant ($z > 0.8$) and highly X-ray luminous clusters of galaxies, Cl J1226.9+3332, Cl J0152.7–1357 and MS 1054.4–0321. Two of the clusters, Cl J1226.9+3332 and Cl J0152.7–1357, were recently discovered in the WARPS X-ray survey. Their high X-ray luminosity suggests they are massive systems and, if confirmed, would provide strong constraints on the cosmological parameters of structure formation models. Our Sunyaev-Zel'dovich Effect data provide confirmation that they are massive clusters similar to the well studied cluster MS 1054.4–0321. Assuming the clusters have the same gas mass fraction derived from SZE measurements of eighteen known massive clusters, we are able to infer their mass and electron temperatures from the SZE data. The derived electron temperatures are $10.0_{-1.5}^{+2.0}$, $8.5_{-1.5}^{+2.0}$, and $10.3_{-2.0}^{+2.5}$ KeV, respectively, and we infer total masses of $\sim 2 \times 10^{14} h_{100}^{-1} M_{\odot}$ within a radius of $65''$ for all three clusters. For Cl J0152.7–1357 and MS 1054.4–0321 we find good agreement between our SZE derived temperatures and those derived from X-ray spectroscopic measurements. No X-ray derived temperatures are available for Cl J1226.9+3332, and thus the SZE data provide the first confirmation that it is indeed a massive system. The demonstrated ability to determine cluster temperatures and masses from SZE observations without access to X-ray data illustrates the power of using deep SZE surveys to probe the distant universe.

Subject headings: cosmology: observations — galaxies: clusters: individual (Cl J1226.9+3332, Cl J0152.7–1357, MS 1054.4–0321) — Sunyaev-Zel'dovich Effect — cosmic microwave background — techniques: interferometric

¹Dept. of Space Science, SD50, NASA Marshall Space Flight Center, Huntsville, AL 35812

²Department of Astronomy and Astrophysics, University of Chicago, Chicago, IL 60637

³Harvard-Smithsonian Center for Astrophysics, 60 Garden Street, Cambridge, MA 02138

⁴Physics Department, University of California, Berkeley, CA 94720

⁵Institute for Astronomy, 2680 Woodlawn Dr., Honolulu, HI 96822

1. Introduction

The existence of galaxy clusters at high redshift can place powerful constraints on the physical and cosmological parameters of structure formation models (e.g. Bahcall & Cen (1992); Luppino & Gioia (1995); Oukbir & Blanchard (1997); Donahue et al. (1998); Eke et al. (1998); Haiman et al. (2000)). The greatest leverage is provided by the most massive and distant clusters (e.g. Viana & Liddle (1996)). Two distant and highly x-ray luminous clusters were recently discovered in the Wide Angle ROSAT Pointed Survey (WARPS⁶): Cl J1226.9+3332 at $z = 0.89$ (Ebeling et al. 2001), and Cl J0152.7–1357 at $z = 0.83$ (Ebeling et al. 2000). Cl J0152.7–1357 was also discovered independently in the RDCS and SHARC surveys (Della Ceca et al. 2000; Romer et al. 2000). Based on their x-ray luminosity ($L_X[0.5–2\text{keV}] \gtrsim 2 \times 10^{44}h_{100}^{-2} \text{ erg s}^{-1}$), these clusters are thought to be highly massive which, if confirmed, will provide significant constraints on cosmological models (Bahcall & Fan 1998).

In this paper, we present interferometric imaging of the Sunyaev-Zeldovich Effect (SZE) in these clusters, which provides a measure of the gas pressure integrated along the line of sight (Sunyaev & Zel'dovich 1972; Birkinshaw 1999). The change in the observed brightness temperature of the Cosmic Microwave Background (CMB) radiation that results from passage through the thermally ionized gas permeating a galaxy cluster is given by

$$\frac{\Delta T_{\text{thermal}}}{T_{\text{CMB}}} = f(\nu) \frac{k_B \sigma_T}{m_e c^2} \int n_e T_e dl$$

where T_{CMB} is the microwave background temperature (2.7 K); σ_T is the Thomson scattering cross section; and m_e , n_e , and T_e are the electron mass, density, and temperature. The frequency dependence of the SZE is represented by $f(\nu)$; in the Rayleigh-Jeans limit, $f(\nu) = -2$. We use the SZE to determine the mass of Cl J1226.9+3332 and Cl J0152.7–1357 using the methods developed by Grego et al. 2001; in addition, we present interferometric SZE data on MS 1054.4–0321, a cluster of known temperature and mass at $z = 0.83$ (Gioia & Luppino 1994; Donahue et al. 1998; Hoekstra et al. 2000), which provides a standard against which the WARPS clusters can be compared.

The SZE observations and data analysis are described in section II, and the conclusions drawn from these data will be found in section III. Throughout this *Letter* we parameterize the Hubble constant in terms of h_{100} , where $H_0 \equiv 100h_{100} \text{ km s}^{-1} \text{ Mpc}^{-1}$. Uncertainties are reported at the 68% confidence level.

⁶Scharf et al. (1997), Jones et al. (1998)

2. Interferometric Imaging of the Sunyaev-Zel'dovich Effect

2.1. Observations

To image the Sunyaev-Zeldovich Effect in these distant clusters, we outfitted the Owens Valley Radio Observatory (OVRO) and Berkeley-Illinois-Maryland-Association (BIMA) millimeter interferometers with sensitive centimeter-wave receivers optimized for SZE measurements (Carlstrom et al. 1996). Our receivers use cryogenically cooled 26-36 GHz high electron mobility transistor (HEMT) amplifiers (Pospieszalski et al. 1995), with characteristic receiver temperatures of $T_{rx} \sim 11\text{-}20$ K at the frequency of 28.5 GHz used for these observations. The cluster pointing centers and on-source integration times are given in Table 1.

The interferometric measurements of Cl J1226.9+3332, and Cl J0152.7–1357 were made at the BIMA interferometer in 1998 and 2000 with nine 6.1 meter antennas in a closely packed configuration to maximize sensitivity to the SZE, with a 6.6' FWHM primary beam and baselines ranging from 0.6 to 14.3 k λ . Typical system temperatures, scaled to above the atmosphere, are $\sim 40\text{-}45$ K in an 800 MHz band centered at 28.5 GHz. Observations of a bright phase calibrator were interleaved with cluster measurements every 25 minutes, and Mars was used for amplitude calibration (Rudy 1987; Grego et al. 2000). The MIRIAD software package (Sault et al. 1995) was used to calibrate and edit the visibility data and to output the reduced data in UVFITS format for subsequent analysis.

The interferometric measurements of MS 1054.4–0321 were made at the OVRO millimeter array in June 1996 with six 10.4 meter antennas in a closely packed configuration, with a 4.2' FWHM primary beam and baselines ranging from 1.0 to 12.0 k λ . Typical system temperatures, scaled to above the atmosphere, are ~ 45 K in two 1 GHz channels centered at 28.5 and 30.0 GHz (2 GHz total bandwidth). Observations of a bright phase calibrator were interleaved with cluster measurements every 24 minutes. The MMA software package (Scoville et al. 1993) was used to calibrate and edit the visibility data and to output the reduced data in UVFITS format for subsequent analysis.

We flagged data from baselines when one of the telescopes was shadowed by another telescope in the array, cluster data that were not bracketed in time by phase calibrator data (mainly at the beginning or end of a track), data for which the phase calibrator indicated poor atmospheric coherence, and, rarely, data with spurious correlations.

2.2. Data Analysis

In order to properly model the cluster, we must account for any point sources in the field. To identify these point sources, we used DIFMAP (Pearson et al. 1994) to produce a high resolution image, using only data from baselines longer than $2 \text{ k}\lambda$. The resulting synthesized beam sizes, RMS noise levels, and point source detections are given in Table 2.

We perform a quantitative analysis of the observed SZE profiles by fitting isothermal β models (Cavaliere & Fusco-Femiano 1976, 1981) and point sources to the interferometric data directly in the Fourier (u, v) plane, where the noise characteristics and the spatial filtering of the interferometer are well understood. The spherical isothermal β model density is described by

$$n_e(r) = n_{eo} \left(1 + \frac{r^2}{r_c^2}\right)^{-3\beta/2}, \quad (1)$$

where the core radius r_c and β are shape parameters, and n_{eo} is the central electron number density. With this model, the SZ Effect temperature decrement is

$$\Delta T(\theta) = \Delta T(0) \left(1 + \frac{\theta^2}{\theta_c^2}\right)^{\frac{1}{2} - \frac{3\beta}{2}}, \quad (2)$$

where $\theta = r/D_A$, $\theta_c = r_c/D_A$, D_A is the angular diameter distance, and $\Delta T(0)$ is the temperature decrement at zero projected radius.

We determine the best-fit point source positions and fluxes, as well as the cluster centroid, using a simplex algorithm which minimizes the chi-squared statistic (Reese et al. 2000). We fix the cluster centroid and the point source positions and fluxes at their best-fit values, and calculate the chi-squared statistic over a large range of θ_c , β , and ΔT_0 values. For a given electron temperature, T_e , the β model then yields the gas density profile $n_e(\theta)$ at each $(\theta_c, \beta, \Delta T_0)$ point. The gas mass and the total cluster mass can be calculated directly from $n_e(\theta)$, assuming that the intracluster medium (ICM) is in hydrostatic equilibrium with the cluster potential. Following the methods outlined in Grego et al. 2001, we calculate the gas mass, total mass, and gas mass fraction over the $(\theta_c, \beta, \Delta T_0)$ grid, and report the total mass values for which the χ^2 statistic is within the 68% confidence interval ($\Delta\chi^2 = 1$). We adopt a fiducial angular radius of $65''$, where our mass determinations are most tightly constrained.

We can estimate the electron temperature directly from the SZE data by finding the range of T_e values that yield a cluster gas mass fraction, f_g , consistent with the mean value measured by Grego et al. (2001) for a sample of eighteen clusters. The mean gas mass fraction found by Grego et al. for a sample of eighteen clusters is $f_g(r_{500}) = 0.081_{-0.011}^{+0.009} h_{100}^{-1}$ (statistical uncertainty at 68% confidence level, assuming an $\Omega_M=0.3$, $\Omega_\Lambda=0.7$ cosmology). To determine

the gas mass fraction at r_{500} for Cl J1226.9+3332, Cl J0152.7–1357, and MS 1054.4–0321, we scale the gas mass fractions measured at $65''$ to r_{500} using relations derived from numerical simulations (Evrard et al. 1996; Evrard 1997), as discussed in Grego et al. (2001). This calculation is repeated for a number of different temperatures ranging from 4–12 keV, and we report the T_e^{SZ} values that are consistent (at the 68% confidence level) with the mean gas mass fraction. The results are insensitive to the adopted cosmology; we repeated the calculations for an $\Omega_M=0.3$ and $\Omega_\Lambda=0.0$, and find that the total mass (and hence T_e^{SZ}) is $\sim 3\%$ lower.

3. Results and Conclusions

Synthesized images of the SZ Effect toward Cl J1226.9+3332, Cl J0152.7–1357, and MS 1054.4–0321 are shown in Fig. 1. The SZE decrement is detected with high significance in all of these distant clusters, and the locations of the SZE and X-ray centroids are consistent (Tables 1 and 3). Using the SZE data and the analysis techniques described in Section 2.2, we determine the temperature and mass of each cluster (Table 3). X-ray temperature measurements for Cl J0152.7–1357 (Della Ceca et al. 2000) and MS 1054.4–0321 (Donahue et al. 1998) are also shown in Table 3, and we find that these X-ray temperature measurements are consistent with the values inferred from the SZE data within the stated uncertainties.

From the SZE data, we infer a total mass of $\gtrsim 2 \times 10^{14} h_{100}^{-1} M_\odot$ within a radius of $65''$ for each of the clusters shown in Table 3. These mass calculations can be checked against values derived from gravitational lensing, X-ray, and optical observations of MS 1054.4–0321 (Donahue et al. 1998; van Dokkum et al. 2000; Hoekstra et al. 2000). Hoekstra et al. (2000) infer a total mass of $5.4 \pm 0.6 \times 10^{14} h_{100}^{-1} M_\odot$ within an aperture of radius $94''$. To compare the SZE and gravitational lensing results, we use $T_e^{SZ}=10.0$ keV and calculate the gas mass within a $94''$ radius aperture to be $M_{gas}^{SZ}(< 94'') = 2.8 \pm 1.5 \times 10^{13} h_{100}^{-2} M_\odot$. Using the gas mass fraction within r_{500} from Section 2.2, we infer the total mass of MS 1054.4–0321 to be $M_{total}^{SZ}(< 94'') = 3.5 \pm 1.5 \times 10^{14} h_{100}^{-1} M_\odot$, consistent with the lensing measurements of Hoekstra et al. (2000).

Based on the SZE data we conclude that the newly-discovered clusters Cl J1226.9+3332 and Cl J0152.7–1357 are highly massive, with a total mass of $M_{total}^{SZ} \gtrsim 2 \times 10^{14} h_{100}^{-1} M_\odot$ within a radius of $65''$. These values are comparable to the mass inferred from SZE imaging of the $z = 0.83$ cluster MS 1054.4–0321, which has been confirmed by X-ray, optical, and gravitational lensing studies. These results demonstrate the ability to determine cluster temperatures and masses from SZE data without access to X-ray data, and illustrates the

power of using deep SZE surveys to probe the distant universe. More precise measures of the temperature and mass of ClJ1226.9+3332 and ClJ0152.7–1357 will be possible with deep X-ray imaging and spectroscopy, which will be obtained within the coming year by the Chandra and XMM X-ray observatories; with these data in hand, the SZE measurements can be used to measure the distance to each cluster (Reese et al. 2000) and to further constrain their density, mass, and gas mass fraction (Grego et al. 2001).

We dedicate this paper to the memory of our friend and colleague Mark Warnock, who freely gave of his expertise and time and made great contributions to the interferometric SZE imaging experiment. We also thank Cheryl Alexander, Rick Forster, Steve Padin, Dick Plambeck, Steve Scott, David Woody, and the staff of the BIMA and OVRO observatories for their outstanding support, and Laurence Jones, Eric Perlman, and Caleb Scharf for providing data on ClJ1226.9+3332 prior to publication. ER gratefully acknowledges support from NASA GSRP Fellowship NGT5-50173. This work is supported by NASA LTSA grants NAG5-7986 (JC,MJ,WH) and NAG5-8253 (HE). Radio astronomy at the BIMA millimeter array is supported by NSF grant AST 96-13998. The OVRO millimeter array is supported by NSF grant AST96-13717. The funds for the additional hardware for the SZE experiment were from a NASA CDDF grant, a NSF-YI Award, and the David and Lucile Packard Foundation.

REFERENCES

Bahcall, N. A. & Cen, R. 1992, *ApJ*, 398, L81
 Bahcall, N. A. & Fan, X. 1998, *ApJ*, 504, 1
 Birkinshaw, M. 1999, *Physics Reports*, 310, 97
 Carlstrom, J. E., Joy, M., & Grego, L. 1996, *ApJ*, 456, L75
 Cavaliere, A. & Fusco-Femiano, R. 1976, *A&A*, 49, 137
 —. 1981, *A&A*, 100, 194
 Della Ceca, R., Scaramella, R., Gioia, I. M., Rosati, P., Fiore, F., & Squires, G. 2000, *A&A*, 353, 498
 Donahue, M., Voit, G. M., Gioia, I., Lupino, G., Hughes, J. P., & Stocke, J. T. 1998, *ApJ*, 502, 550
 Ebeling, H., Jones, L. R., Fairley, B. W., Perlman, E., Scharf, C., & Horner, D. 2001, *ApJ*, submitted
 Ebeling, H., Jones, L. R., Perlman, E., Scharf, C., Horner, D., Wegner, G., Malkan, M., Fairley, B. W., & Mullis, C. R. 2000, *ApJ*, 534, 133
 Eke, V. R., Cole, S., Frenk, C. S., & Patrick Henry, J. 1998, *MNRAS*, 298, 1145
 Evrard, A. E. 1997, *MNRAS*, 292, 289
 Evrard, A. E., Metzler, C. A., & Navarro, J. F. 1996, *ApJ*, 469, 494
 Gioia, I. M. & Luppino, G. A. 1994, *ApJS*, 94, 583
 Grego, L., Carlstrom, J., Reese, E., Holder, G., Holzapfel, W., Joy, M., Mohr, J., & Patel, S. 2001, *ApJ*–submitted
 Grego, L., Carlstrom, J. E., Joy, M. K., Reese, E. D., Holder, G. P., Patel, S., Cooray, A. R., & Holzapfel, W. L. 2000, *ApJ*, 539, 39
 Haiman, Z., Mohr, J. J., & Holder, G. P. 2000, *ApJ*, submitted
 Hoekstra, H., Franx, M., & Kuijken, K. 2000, *ApJ*, 532, 88
 Jones, L. R., Scharf, C., Ebeling, H., Perlman, E., Wegner, G., Malkan, M., & Horner, D. 1998, *ApJ*, 495, 100
 Luppino, G. A. & Gioia, I. M. 1995, *ApJ*, 445, L77
 Neumann, D. M. & Arnaud, M. 2000, submitted
 Oukbir, J. & Blanchard, A. 1997, *A&A*, 317, 1
 Pearson, T. J., Shepherd, M. C., Taylor, G. B., & Myers, S. T. 1994, *BAAS*, 185, 0808
 Pospieszalski, M. W., Lakatos, W. J., Nguyen, L. D., Lui, M., Liu, T., Le, M., Thompson, M. A., & Delaney, M. J. 1995, *IEEE MTT-S Int. Microwave Symp.*, 1121
 Reese, E. D., Mohr, J. J., Carlstrom, J. E., Joy, M., Grego, L., Holder, G. P., Holzapfel, W. L., Hughes, J. P., Patel, S. K., & Donahue, M. 2000, *ApJ*, 533, 38
 Romer, A. K., Nichol, R. C., Holden, B. P., Ulmer, M. P., Pildis, R. A., Merrelli, A. J., Adami, C., Burke, D. J., Collins, C. A., Metevier, A. J., Kron, R. G., & Commons, K. 2000, *ApJS*, 126, 209

Rudy, D. J. 1987, PhD thesis, California Inst. of Tech., Pasadena.

Sault, R. J., Teuben, P. J., & Wright, M. C. H. 1995, ASP Conf. Ser. 77: Astronomical Data Analysis Software and Systems IV, 4, 433

Scharf, C. A., Jones, L. R., Ebeling, H., Perlman, E., Malkan, M., & Wegner, G. 1997, ApJ, 477, 79

Scoville, N. Z., Carlstrom, J. E., Chandler, C. J., Phillips, J. A., Scott, S. L., Tilanus, R. P. J., & Wang, Z. 1993, PASP, 105, 1482

Sunyaev, R. A. & Zel'dovich, Y. B. 1972, Comments Astrophys. Space Phys., 4, 173

van Dokkum, P. G., Franx, M., Fabricant, D., Illingworth, G. D., & Kelson, D. D. 2000, ApJ, 541, 95

Viana, P. T. P. & Liddle, A. R. 1996, MNRAS, 281, 323

Table 1. Cluster Observation Log

Cluster Name	redshift	Pointing Center (J2000)		On-source Integ. time (hours)
		α	δ	
Cl J1226.9+3332	0.89	12 ^h 26 ^m 58 ^s .0	33°32'45" ^a	41.6
Cl J0152.7–1357	0.83	01 ^h 52 ^m 43 ^s .0	–13°57'29" ^b	27.8
MS 1054.4–0321	0.83	10 ^h 56 ^m 59 ^s .5	–03°37'28" ^c	43.0

^aPointing center coincident with X-ray cluster center from Ebeling et al. (2001).

^bPointing center coincident with X-ray cluster center from Ebeling et al. (2000).

^cPointing center coincident with optical cluster center from Gioia & Luppino (1994). The ROSAT/HRI X-ray center is at 10^h56^m58^s.6, –03°37'36" (Neumann & Arnaud 2000).

Table 2. Radio Point Sources

Cluster Name	Synth. Beam ($r_{uv} > 2k\lambda$)	RMS noise (mJy/beam)	$\Delta\alpha$ (arcsec)	$\Delta\delta$ (arcsec)	Observed Flux (mJy)
Cl J1226.9+3332	$14.1'' \times 16.1''$	0.152	260.0	-39.3	1.73
Cl J0152.7-1357	$13.7'' \times 23.1''$	0.221	—	—	—
MS 1054.4-0321	$17.4'' \times 23.3''$	0.092	0.1	1.4	0.98
			-161.0	1.9	0.63
			-25.5	-86.9	0.35

Table 3. Cluster Properties derived from SZE measurements

Cluster Name	<u>Cluster Position</u> ^a $\Delta\alpha$	T_e^{Xray} $\Delta\delta$	T_e^{SZE} (keV)	$M_{total} < 65''$ ($10^{14} h^{-1} M_\odot$)
Cl J1226.9+3332	0.''2	12.''3	—	$10.0^{+2.0}_{-1.5}$
Cl J0152.7-1357	-1.''8	-9.''2	$6.5^{+1.7}_{-1.2}$	$8.5^{+2.0}_{-1.5}$
MS 1054.4-0321	-7.''8	-5.''3	$12.3^{+3.1}_{-2.2}$	$10.3^{+2.5}_{-2.0}$

^aOffsets from radio pointing center (Table 1)

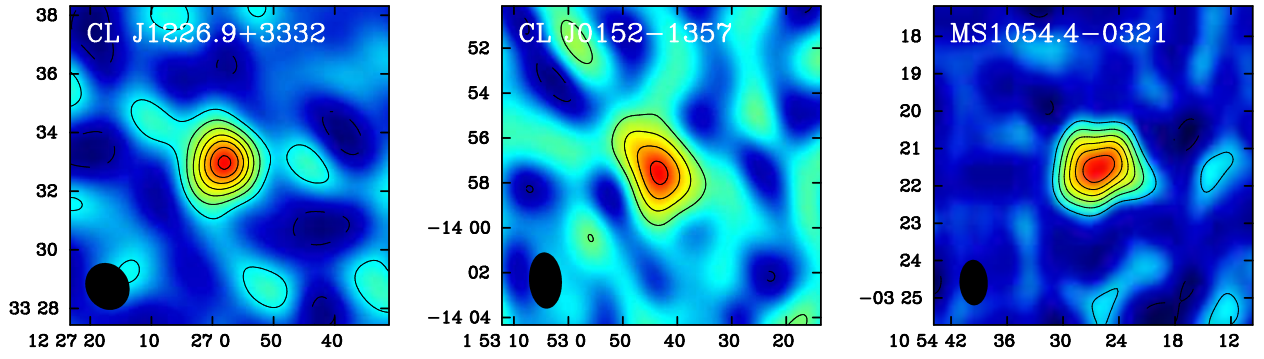


Fig. 1.— Synthesized images of the SZE decrement in CL J1226.9+3332, CL J0152.7–1357, and MS 1054.4–0321. Left panel: The resolution is $99.3'' \times 87.4''$ at position angle (p.a.) 32° , resulting from a Gaussian taper applied to the u - v data at half-power radius $1 \text{ k}\lambda$. Contours are multiples of $290 \mu\text{Jy beam}^{-1}$ (1.5σ), and the rms is $190 \mu\text{Jy beam}^{-1}$. Center panel: The resolution is $151'' \times 87''.9$ at p.a. 4° , resulting from a Gaussian taper applied to the u - v data at half-power radius $1 \text{ k}\lambda$. Contours are multiples of $480 \mu\text{Jy beam}^{-1}$ (1.5σ), and the rms is $320 \mu\text{Jy beam}^{-1}$. Right panel: The resolution is $73''.1 \times 45''.5$ at p.a. 2° , resulting from a Gaussian taper applied to the u - v data at half-power radius $2 \text{ k}\lambda$. Contours are multiples of $120 \mu\text{Jy beam}^{-1}$ (1.5σ), and the rms is $80 \mu\text{Jy beam}^{-1}$.